Chapter 7 – MODELLING OF WIRE-LINE TRANSMISSION SYSTEMS AS HF NOISE SOURCES

In this Chapter, the general foundation of modelling wire-line transmission systems is presented. In Section 7.1, the principal aspects or mechanisms of the radiated power is addressed, including results from studies and measurement projects. In Section 7.2, the rigorous theoretical basis of PLT modelling by means of dipoles is outlined. In Section 7.3, radiated power estimation from measured electric field is presented. In Section 7.4, the distance conversion factor near a PLT is investigated and compared with measured results. Finally, in Section 7.5, representative PLT sources are listed.

7.1 PRINCIPAL ASPECTS OF THE RADIATED POWER IN THE FAR-FIELD

Figure 7.1-1 shows a simplified model of a wire-line transmission system. The transmitter (PLT or xDSL) injects the signal differentially between two wires, with a power spectral density (PSD) measured in units of dBm/Hz. With an ideal transmission line, there would be no common mode (CM) signal relative to ground caused by the differentially injected signal, but in reality there is. The ratio between CM and differential mode (DM) signal is given by the Common Mode Rejection Ratio (CMRR) or Longitudinal Conversion Loss (LCL). For the differential signal the contribution from the two wires will cancel out in the far-field. This is not the case for the CM signal, which therefore will be the most prominent radiation source.

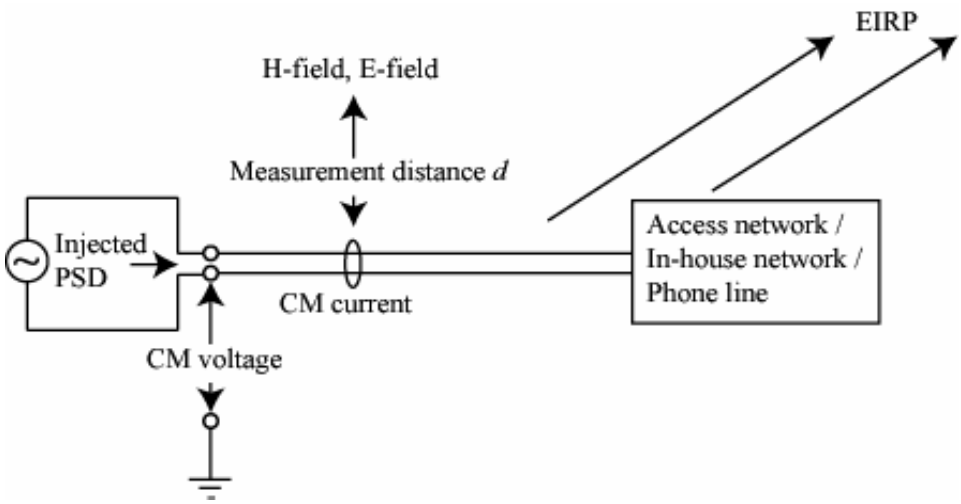

Figure 7.1-1: Simplified Model of a Wire-Line Transmission System, including Quantities Relevant to Far-Field Radiation.

The CM signal consists of a CM current and CM voltage propagating along the line. The ratio between the two is given by the common mode impedance, and the return path for the CM current is through ground. The proposed PLT regulations in Europe define an upper limit on the CM current. In case of reflections and standing waves, caused by impedance discontinuities in the network, the measured CM current level will be different at different positions along the line.

The radiation limits in the German NB30 and the US FCC Part 15 are defined as the field strength at a measurement distance *d* of 3 m and 10 m, respectively. Even though the limit is defined as an electrical field strength in units of dBμV/m (in a specified measurement bandwidth), the actual measurement

procedures below 30 MHz *by definition* measure the magnetic field strength and converts the number to an electric field strength using the far-field free-space impedance of $Z_0 = 120\ \pi$ ohms. Even though this relationship is not exact in the near field, it may still be a good indicator of the ratio between the *maximum* electric and magnetic field strengths [94].

The quantity of interest when considering cumulative effects in the far-field is the EIRP (equivalent (or effective) isotropic radiated power) per unit bandwidth caused by each signal source, in units of dBm/Hz, at different frequencies. The radiation pattern might also be of interest in some cases, but when summing up many different sources with different wiring geometries over a wide area, it is reasonable to approximate the average radiation pattern as isotropic in elevation as well as in azimuth [61],[89]. In the following sections we discuss how the EIRP can be estimated based on available information on injected PSD, CM current, or field strength at some measurement distance.

7.1.1 Antenna Gain Measurements

The antenna gain of a wire-line transmission system is defined as the ratio between EIRP and injected power. For power line systems, several measurement results are reported in the literature, using two principally different measurement methods:

- One method is to inject a signal of known power onto the line and measure the received signal strength at horizontal distances of some km (with ground wave propagation) or overhead in an airplane (with direct wave propagation). Adding the estimated path loss (using GRWAVE or free-space formulas, respectively) to the received signal strength gives an estimate of the EIRP directly. The uncertainty related to the path loss estimate is higher for ground wave than for direct wave.
- The other method is to use the power network as a receiver antenna for remote broadcast transmissions and measure the received signal strength at the injection point. This measurement can be compared with a simultaneous collocated measurement of the same broadcast signal using a calibrated reference antenna, and the difference between the two measurements compared to reference antenna gain gives the antenna gain directly. Assuming reciprocity of the radio channel and power line network, the receive antenna gain is equal to the transmit antenna gain. This method is easier than the first method, but the measurements can only be conducted at frequencies and directions given by the broadcast transmitters.

Ref. [55] assumes the antenna gain for power line systems to be –20 dBi, referring to airborne measurements.

Ref. [57] reports measured antenna gains in the range –20 dBi to –50 dBi, based on received broadcast signals. The measurements close to –20 dBi were for In-House systems, while those close to –50 dBi were for underground Access cables.

Ref. [58] reports measured antenna gains in the range –30 dBi to –50 dBi, based on measured ground wave radiation. The measurements close to –30 dBi were for In-House systems, while those close to –50 dBi were for underground Access cables.

Ref. [59] reports antenna gains for In-House systems to be approximately –30 dBi, based on received broadcast signals.

Ref. [60] estimates the measured gain of a sample house wiring to be in the range –20 to –30 dBi, based on radiated measurements 10 m from the wall outside the house.

Reference [61] mentions a worst-case antenna gain for power line systems of –15 dBi.

Measurements with 9 kHz bandwidth presented in [68] over a wide range of European power line networks show that on average an injected power level of 0 dBm leads to an electrical field strength of about 60 dBμV/m at 3 m measurement distance.

Gain measurements of In-House grids by the university of Karlsruhe [7, p. 83], based on received broadcast signals, show mean values of –40 dBi for f < 10 MHz and –30 dBi for f > 10 MHz.

According to discussions cited in minutes from a SE35 meeting in 2001 [66], "It was generally felt that this gain is in the order of –20 dBi for aerial cables and of –30 to –40 dBi for buried cables."

Based on these references, the Task Group recommends using the following antenna gains:

- –30 dBi for In-House systems;
- –15 dBi for overhead Access systems; and
- –50 dBi for underground Access systems.

It should be recognized that there are uncertainties in these numbers of the order of ±5 to ±10 dB due to statistical spread. Furthermore, in the case of overhead Access system power lines, at resonant frequencies the antenna gain may be higher by 10 – 13 dB [73].

7.1.2 CMRR/LCL Measurements

CMRR/LCL values are generally measured as the ratio between the DM and CM voltages *at the injection point*. This may not be a representative measurement with respect to radiation, since impedance mismatches and standing waves can cause large variations in the CM current along the line.

A measurement procedure for LCL of PLT systems is presented in [95].

Measurements presented in [67] over a wide range of European power line networks show average LCL values of about 30 dB.

Measurements presented in [69] show large variations in the CM current at different positions in a house (and also at different frequencies). For an injected power level of about 0 dBm the CM current varies between 10 dBμA and –30 dB dBμA at the same frequency.

Simulation results presented in [65] indicate that, for the case of a single straight power line with no branches, a LCL of 24 dB (asymmetrical loading) will cause the radiated power to increase by 50 – 70 dB compared to symmetrical loading. For more complicated network geometries, the increase in radiation due to asymmetrical loading is similar for low HF frequencies and higher for high HF frequencies. According to [70], the CM currents along the line can not be deduced from the CM signal at the feed point due to this kind of variations, and therefore the LCL can not directly be used to estimate the radiated fields in case of PLC. Similar arguments are given in [71].

7.1.3 Numerical Methods

Several works have used numerical methods, e.g., Numerical Electromagnetic Code (NEC), to model radiation from wire-line networks. Based on a modelled network geometry and signal injection point, it is possible to compute the field strength at any point in space, the CM current at any point along the line, and the far-field radiation in all directions. This approach is very exact if the model is realistic, and can give direct estimates of the ratio between EIRP and field strength at measurement distance, or between EIRP and common mode current.

The downside to this approach is that it only gives results for a single geometry, and general conclusions may be hard to draw. An example of general conclusions is found in [61], which reported that summation of radiation patterns of NEC models for a large number of houses in London gives an average radiation pattern that is close to isotropic in azimuth as well as in elevation (at 90° elevation the radiation pattern is 6 dB below the maximum).

In [73], a detailed simulation of an example overhead wiring geometry is presented, using an FDTD (finite difference time domain) method. Among other things, this simulation predicts that an injected power spectral level of –50 dBm/Hz can give rise to field strength levels of 65 dBμV/m at a distance d = 10 m from the line, in a 3.5 kHz measurement bandwidth in the frequency range 21 – 24 MHz. This corresponds to a PSD (EIRP/Hz) of –55.2 dBm/Hz, or an equivalent antenna gain of –5.2 dBi. This value is higher than the recommended –15 dBi, but it is not known if the wiring geometry was resonant at the frequency of simulation. However, it is within the aforementioned uncertainty criteria.

Other numerical simulations of PLT systems are found in [96],[97].

7.1.4 Ampere's Law

For the case of a static (DC) common mode current on a long straight wire, the relationship between the CM current I_{CM} and the magnetic field H at measurement distance d would be given by Ampere's law (or from the Biot-Savart law): $H(d) = I_{CM} / 2\pi d$.

For alternating fields, this formula is not exact, but is a good approximation only for $d << \lambda$. It was used by the European JWG when converting field strength limits to CM current limits.

7.1.5 Impedance Discontinuities

In Annex 4 of [3] expressions are developed in the far-field, for the relationship between the EIRP and the field strength measured with a magnetic loop, at a measurement distance d, assuming that the radiation source is a small electric or magnetic dipole (in theory infinitesimal, in practice very small compared to the wavelength). These may be good models for radiation caused by impedance discontinuities, but are obviously inexact for radiation from long wires.

The derivations assume that the field strength is measured using a magnetic loop antenna and converted to electric field E(d), in units of V/m, using the free-space impedance of 120 π ohms (by definition).

Assuming a small electric dipole, the relationship is shown to be

$$\mathrm{EIRP} = \frac{d^4}{d^2 + \left(\frac{\lambda}{2\pi}\right)^2} \frac{\left[E(d)\right]^2}{30} \tag{7-1}$$

Assuming a small magnetic dipole, the relationship is shown to be

$$\mathrm{EIRP} = \frac{d^6}{\left(\frac{\lambda}{2\pi}\right)^4 - \left(\frac{\lambda}{2\pi}\right)^2 d^2 + d^4} \frac{\left[E(d)\right]^2}{30} \tag{7-2}$$

where E(d) is in V/m, d and λ are in metres, 30 is in ohms, and EIRP is in Watts.

Figures in Annex 4 of [3] show that for d = 3 m, the two models are relatively close (within 3 dB) above 8 MHz, but differ by 15 dB at 3 MHz (the electric dipole model predicting the highest EIRP). For d = 10 m, the difference between the two models is within 3 dB in the entire HF frequency range.

If this approach is applied, it is recommended that the above formula (7-1) for an electric dipole be used, since power lines are more likely to behave as electric than magnetic antennas. However, it should be noted that this formula is inexact for radiation from wires of length comparable to the wavelength, or longer. The approach is therefore likely to be more suitable for In-House systems than for Access systems. For overhead PLT lines of Access systems, the expression given in Section 7.3 is the appropriate one.

7.2 PLT LINE MODELLING TECHNIQUES WITH DIPOLES

In modelling the emissions from a PLT line, one of the best techniques is to model the PLT wires as a successive set of dipoles, assuming that the standing waves present are the dominant emission source. As the PLT is basically a wire, the dipole is the nearest model to a wire. To implement such an approach, the dipole formulation needs to be addressed first. As to the dipole type, both half-wavelength and one-wavelength dipoles are suitable; however, the half-wavelength has the wider half-power beamwidth (78 degrees vs. 48 degrees), therefore it is preferable (the wider the beamwidth, the smoother the pattern overlap).

There are two main issues:

a) the determination of the field strength roll-off with respect to distance away from the PLT (the distance conversion factor); and

b) the general profile of the field strength at various distances away from the PLT in order to assess the interference effects.

It should be noted that the following modelling techniques apply to overhead Access PLT systems. In-House systems contain both vertical and horizontal lines. To model these lines, numerical electromagnetic computational models have to be used. In view of the great variety of in-house wiring geometries, a universal model is not possible. Therefore, measurement results obtained by various groups are used (see Section 7.4.1).

7.2.1 Exact Solution of a Dipole

The exact solution of a dipole, valid at any distance in both near-field and far-field, can be carried out by means of the geometry shown in Figure 7.2.1-1. Given the PLT geometry, the cylindrical coordinate system is more practical in this case rather than the spherical coordinate system generally used in electromagnetics.

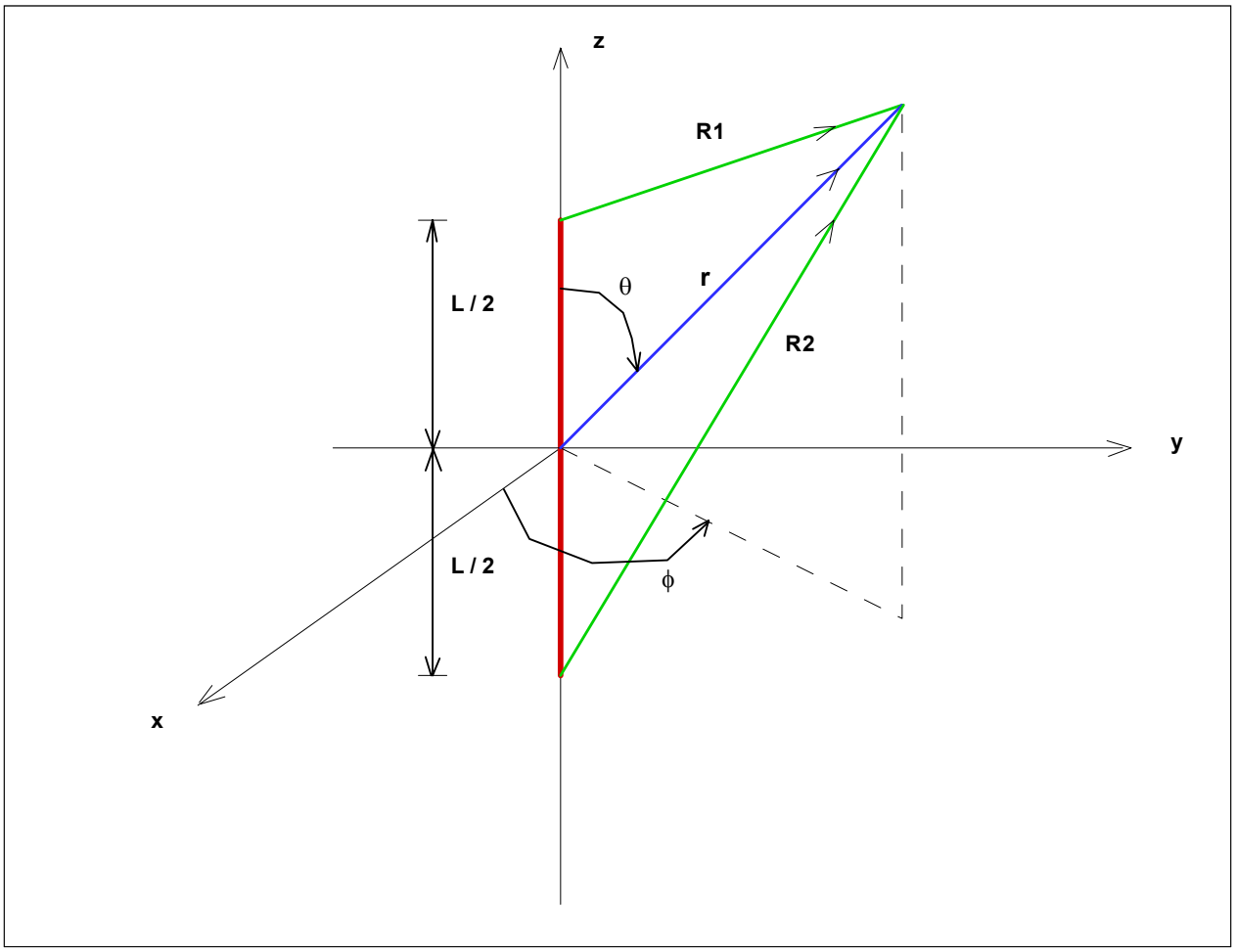

Figure 7.2.1-1: The Geometry of Dipole used in the Derivation of Fields.

Assuming a sinusoidal current distribution along each half of a dipole of any length L, along the z-coordinate axis:

$$
\begin{aligned}
I(x',y',z') &= I_0 \sin\left(k\left(\frac{L}{2}-z'\right)\right)\hat{z} \qquad 0 \le z' \le \frac{L}{2} \\
I(x',y',z') &= I_0 \sin\left(k\left(\frac{L}{2}+z'\right)\right)\hat{z} \qquad -\frac{L}{2} \le z' \le 0
\end{aligned}
\tag{7-3}
$$

where k is the free-space wave number (or propagation constant) and is given by: $k = \frac{2\pi}{\lambda}$, and I_0 is the line current.

In cylindrical coordinates, the field components are then represented by the following exact solution expressions [81]. Similar expressions can also be found in older texts [82], [83].

$$H_\phi = j\frac{I_0}{4\pi\rho}\left(e^{-jkR1} + e^{-jkR2} - 2\cos\left(\frac{kL}{2}\right)e^{-jkr}\right) \tag{7-4}$$

$$E_\rho = j\frac{\eta I_0}{4\pi\rho}\left(\left(z-\frac{L}{2}\right)\frac{e^{-jkR1}}{R1} + \left(z+\frac{L}{2}\right)\frac{e^{-jkR2}}{R2} - 2z\cos\left(\frac{kL}{2}\right)\frac{e^{-jkr}}{r}\right) \tag{7-5}$$

$$E_z = -j\frac{\eta I_0}{4\pi}\left(\frac{e^{-jkR1}}{R1} + \frac{e^{-jkR2}}{R2} - 2\cos\left(\frac{kL}{2}\right)\frac{e^{-jkr}}{r}\right) \tag{7-6}$$

where ρ is the radial part of cylindrical coordinates (ρ,ϕ,z), and η is the intrinsic impedance of free-space.

R1, R2 and r are given by:

$$R1 = \left(x^2 + y^2 + \left(z - \frac{L}{2}\right)^2\right)^{\frac{1}{2}} \tag{7-7}$$

$$R2 = \left(x^2 + y^2 + \left(z + \frac{L}{2}\right)^2\right)^{\frac{1}{2}} \tag{7-8}$$

$$r = \left(x^2 + y^2 + z^2\right)^{\frac{1}{2}} \tag{7-9}$$

The radial component of the electric field E_ρ dies out quickly away from the antenna. The electric field along the z axis, E_z is the field that will be used in the modelling.

7.2.2 Field Computation Far Away from the PLT

The electric field E_z far away from the PLT can be determined by applying the far-field approximations to equation (7-6), as follows:

For amplitude: R1 ≈ R2 ≈ r; for phase: R1 = r – (L/2)cosθ and R2 = r + (L/2)cosθ. Then we obtain:

$$E_z = -j\frac{\eta I_0 e^{-jkr}}{2\pi r}\left(\cos\left(\frac{kL}{2}\cos\theta\right) - \cos\left(\frac{kL}{2}\right)\right) \tag{7-10}$$

Further, applying the cylindrical-spherical relationship z = rcosθ, we obtain,

$$E_z = -j\frac{\eta I_0 e^{-jkr}}{2\pi r}\left(\cos\left(\frac{kLz}{2r}\right) - \cos\left(\frac{kL}{2}\right)\right) \tag{7-11}$$

Alternately, one can apply the spherical-to-cylindrical coordinate transformation to the dipole electric field far-field expressions available in any textbook on antennas, namely:

$$E_z = E_r \cos\theta - E_\theta \sin\theta \tag{7-12}$$

E_r is approximately zero in the far-field, while in spherical coordinates E_θ in the far-field is given by:

$$E_\theta = j\frac{\eta I_0 e^{-jkr}}{2\pi r}\left(\frac{\cos\left(\frac{kL}{2}\cos\theta\right) - \cos\left(\frac{kL}{2}\right)}{\sin\theta}\right) \tag{7-13}$$

Therefore, multiplication of (7-13) by –sin θ will yield (7-10).

7.2.3 Half-Wavelength Dipole Model

The electric field general exact solution and the far-field approximation solution expressions in cylindrical coordinates are given by (7-6) and (7-11) respectively. For the half-wavelength dipole model, equivalent expressions can be obtained readily by substituting λ/2 for L. Thus, $\frac{kL}{2} = \frac{1}{2} * \frac{2\pi}{\lambda} * \frac{\lambda}{2} = \frac{\pi}{2}$ and $\cos\left(\frac{kL}{2}\right) = \cos\left(\frac{\pi}{2}\right) = 0$.

Therefore, we obtain,

$$E_z = -j\frac{\eta I_0}{4\pi}\left(\frac{e^{-jkR1}}{R1} + \frac{e^{-jkR2}}{R2}\right) \tag{7-14}$$

for the exact solution case, and

$$E_z = -j\frac{\eta I_0 e^{-jkr}}{2\pi r}\cos\left(\frac{\pi z}{2r}\right) \tag{7-15}$$

for the far-field approximation case.

7.2.4 One-Wavelength Dipole Model

Similarly, for the one-wavelength dipole model, equivalent expressions can be obtained readily by substituting λ for L in (7-6) and (7-11). Thus, $\frac{kL}{2} = \frac{1}{2} * \frac{2\pi}{\lambda} * \lambda = \pi$ and $\cos\left(\frac{kL}{2}\right) = \cos(\pi) = -1$.

$$E_z = -j\frac{\eta I_0}{4\pi}\left(\frac{e^{-jkR1}}{R1} + \frac{e^{-jkR2}}{R2} + 2\frac{e^{-jkr}}{r}\right) \tag{7-16}$$

for the exact solution case, and

$$E_z = -j\frac{\eta I_0 e^{-jkr}}{2\pi r}\left(\cos\left(\frac{\pi z}{r}\right) + 1\right) \tag{7-17}$$

for the far-field approximation case.

7.2.5 Small Dipole Model

While modelling PLTs with small dipoles is not recommended, in the interest of completeness, exact expressions for small dipoles are provided in this section. The criterion defining small dipoles is $\frac{\lambda}{50} \le L \le \frac{\lambda}{10}$.

In spherical coordinates, the exact solutions for the electric and magnetic fields are given by:

$$H_\phi = \frac{I_o L \sin\theta}{8\pi r}\left(jk + \frac{1}{r}\right)e^{-jkr} \tag{7-18}$$

$$E_r = -j\frac{2 I_o \eta L \cos\theta}{8\pi k r^2}\left(jk + \frac{1}{r}\right)e^{-jkr} \tag{7-19}$$

$$E_\theta = j\frac{I_o \eta L \sin\theta}{8\pi k r}\left(k^2 - j\frac{k}{r} - \frac{1}{r^2}\right)e^{-jkr} \tag{7-20}$$

Because the cylindrical coordinates are more suitable to the PLT geometry, the exact electric field component E_z, valid at any distance, can be obtained by means of spherical-to-cylindrical coordinate transformation using (7-12), and the spherical-cylindrical relationships ρ = rsinθ and z = rcosθ.

$$E_z = -j\frac{I_o \eta L}{8\pi r^3}\left(k\rho^2 + \left(\frac{2z^2 - \rho^2}{r}\right)\left(j + \frac{1}{kr}\right)\right)e^{-jkr} \tag{7-21}$$

For the far-field approximation case, this simplifies to:

$$E_z = -j\frac{I_o \eta L k \rho^2}{8\pi r^3} e^{-jkr} \tag{7-22}$$

7.2.6 The Two-Ray Method

In the vicinity of the PLT, the proper determination of the conversion factor with distance requires that the reflected field from the ground be also taken into consideration. Therefore, the best method for such an assessment is the two-ray method illustrated in Figure 7.2.6-1. The proper application of the method in conjunction with E_z is illustrated in Figure 7.2.6-2.

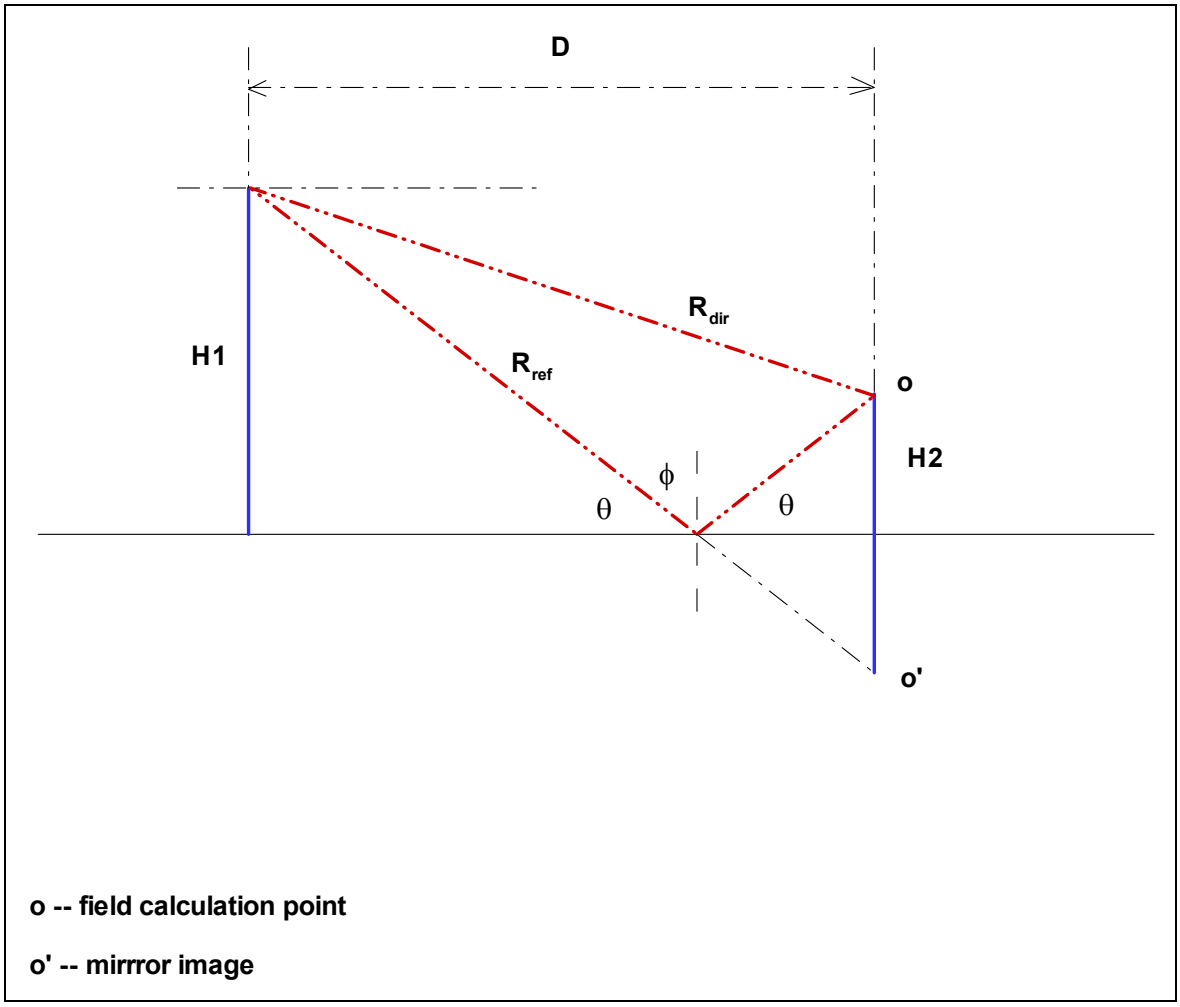

Figure 7.2.6-1: The Two-Ray Field Calculation Geometry.

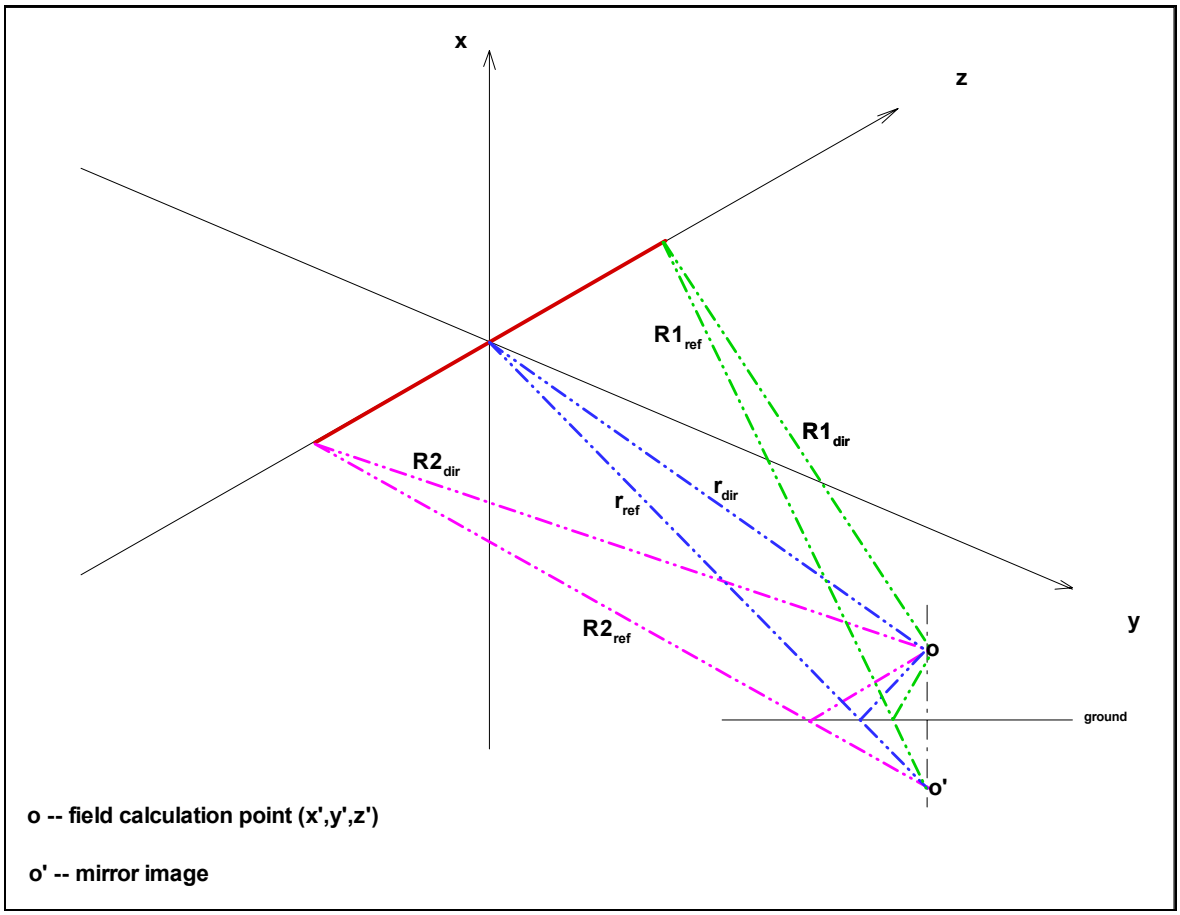

Figure 7.2.6-2: The Two-Ray Field Calculation Geometry near Dipole for Modelling PLT.

In any investigation involving the determination of electromagnetic field strength variation with respect to distance from the source, it is best to work with the geometry that yields the maximum field values. In this case, the maximum value of E_z occurs at z = 0 in cylindrical coordinates (in spherical coordinates, for E_θ this occurs at θ = 90 degrees). In aperture antennas, which are highly directive, this is called the antenna boresight. For a dipole, the term is used loosely to indicate the maximum field strength direction. The height above ground is represented by the x-coordinate, while the horizontal distance away from the dipole (PLT) is represented by the y-coordinate.

When we choose the boresight case for maximum E_z , z = 0, and R1, R2 and r expressions of Section 7.2.1 reduce to:

$$r = \left(x^2 + y^2\right)^{\frac{1}{2}} \tag{7-23}$$

$$R1 = R2 = \left(x^2 + y^2 + \frac{L^2}{4}\right)^{\frac{1}{2}} = \left(r^2 + \frac{L^2}{4}\right)^{\frac{1}{2}} \tag{7-24}$$

From the simple geometry of Figure 7.2.6-1, where the dipole is placed at height H1 and pointing into the page, we have:

$$R_{dir} = \left(D^2 + (H1 - H2)^2\right)^{\frac{1}{2}} \tag{7-25}$$

$$R_{ref} = \left(D^2 + (H1 + H2)^2\right)^{\frac{1}{2}} \tag{7-26}$$

$$\sin\phi = \frac{D}{R_{ref}} \tag{7-27}$$

$$\cos\phi = \frac{H1 + H2}{R_{ref}} \tag{7-28}$$

In adapting the expressions (7-23) through (7-28) to the geometry of the dipole-modelled PLT shown in Figure 7.2.6-2, we can either place the origin point (0,0,0) on the dipole above ground, or we can place the origin point on the ground. For ease of arithmetic and typography, the latter option is preferable.

The dipole-modelled PLT is located at x = H1, the field calculation point is located at x = H2, and the horizontal distance from the PLT is located at y = D. Then we have,

$$r_{dir} = \left((H1 - H2)^2 + D^2\right)^{\frac{1}{2}} \tag{7-29}$$

$$r_{ref} = \left((H1 + H2)^2 + D^2\right)^{\frac{1}{2}} \tag{7-30}$$

$$R1_{dir} = R2_{dir} = \left((H1 - H2)^2 + D^2 + \frac{L^2}{4}\right)^{\frac{1}{2}} = \left(r_{dir}^2 + \frac{L^2}{4}\right)^{\frac{1}{2}} \tag{7-31}$$

$$R1_{ref} = R2_{ref} = \left((H1 + H2)^2 + D^2 + \frac{L^2}{4}\right)^{\frac{1}{2}} = \left(r_{ref}^2 + \frac{L^2}{4}\right)^{\frac{1}{2}} \tag{7-32}$$

The total field at the point of calculation is the sum of direct field plus the product of the reflected field with the proper reflection coefficient. Referring to Figure 7.2.6-1, as E_z is perpendicular to the plane of incidence, i.e., the page, or in other words, parallel to the surface of incidence, i.e., the ground, the proper reflection coefficient is the horizontal reflection coefficient. In an air/ground medium, this is given by:

$$\Gamma_H = \frac{\left(\frac{j\omega\mu_0}{\sigma + j\omega\varepsilon_0\varepsilon_r}\right)^{\frac{1}{2}} \cos\phi - \left(\left(\frac{\mu_0}{\varepsilon_0}\right)\left(1 + \frac{\omega^2\mu_0\varepsilon_0 \sin^2\phi}{j\omega\mu_0\left(\sigma + j\omega\varepsilon_0\varepsilon_r\right)}\right)\right)^{\frac{1}{2}}}{\left(\frac{j\omega\mu_0}{\sigma + j\omega\varepsilon_0\varepsilon_r}\right)^{\frac{1}{2}} \cos\phi + \left(\left(\frac{\mu_0}{\varepsilon_0}\right)\left(1 + \frac{\omega^2\mu_0\varepsilon_0 \sin^2\phi}{j\omega\mu_0\left(\sigma + j\omega\varepsilon_0\varepsilon_r\right)}\right)\right)^{\frac{1}{2}}} \tag{7-33}$$

This can be simplified to:

$$\Gamma_H = \frac{\cos\phi - \left(\left(\varepsilon_r - \sin^2\phi\right) - j\frac{\sigma}{\omega\varepsilon_0}\right)^{\frac{1}{2}}}{\cos\phi + \left(\left(\varepsilon_r - \sin^2\phi\right) - j\frac{\sigma}{\omega\varepsilon_0}\right)^{\frac{1}{2}}} \tag{7-34}$$

Finally, by the substitution of (7-27) and (7-28) we have:

$$\Gamma_H = \frac{\left(\frac{H1 + H2}{r_{ref}}\right) - \left(\left(\varepsilon_r - \left(\frac{D}{r_{ref}}\right)^2\right) - j\frac{\sigma}{\omega\varepsilon_0}\right)^{\frac{1}{2}}}{\left(\frac{H1 + H2}{r_{ref}}\right) + \left(\left(\varepsilon_r - \left(\frac{D}{r_{ref}}\right)^2\right) - j\frac{\sigma}{\omega\varepsilon_0}\right)^{\frac{1}{2}}} \tag{7-35}$$

The proper values of ε_r and σ for a particular location of assessment can be obtained from [28] and [80].

The total field at any point is:

$$E_z^{total} = E_z^{dir} + \Gamma_H E_z^{ref} \tag{7-36}$$

where the appropriate expressions (7-29) to (7-32) are used in equation (7-6). Also,

$$\left|E_z^{total}\right| = \left(E_z^{total} \times \left(E_z^{total}\right)^*\right)^{\frac{1}{2}} \tag{7-37}$$

It should be noted that the two-ray method is only useful within a short distance, perhaps up to 200 metres, given typical PLT line heights (10 – 15 m), and frequencies in the HF range. There are two reasons for this: one theoretical, the other practical. In the first case, ignoring the ground irregularities, at large

distances the grazing angle θ in Figure 7.2.6-1 will become very small, causing the value of the horizontal reflection coefficient to approach –1, and the direct and reflected path lengths to become comparable; all of these effects will cause the total field E_z to approach zero. In the second case, due to many obstacles in and around the wires, the field will not maintain its original polarization indefinitely. Therefore, beyond 200 metres, and also for cases involving skyward propagation of E field, it is advisable to compute the total field E_z by applying a single-ray approach, using equation (7-11). Again, the magnitude of the total field can be computed as before by means of equation (7-37).

7.2.7 Rationale and Justification for Using Exact Dipole Solution Expressions in the Vicinity of the Overhead PLT Line

As stated before, in the vicinity of the PLT and including the near-field, proper modelling is very important. This can only be implemented by using the exact solution expressions when the PLT is modelled by dipoles, because these expressions yield correct results for cases involving the near-field. A comparison of the respective results obtained by the exact solution and the far-field approximation expressions in the vicinity of a PLT will be illustrative.

Again, the boresight case is applied (z = 0) which yields the maximum E_z values. The line current I_0 is 1 ampere. Both half-wavelength (half-wave or λ/2) and one-wavelength (full-wave or λ) dipoles are modelled.

When z = 0, R1 = R2 = R and is given by (7-24), and r is the radial distance from the centre of the dipole, in the boresight direction, and is given by (7-23). L is the dipole length.

7.2.7.1 Half-Wave Dipole Results

For the above set-up, the exact solution given by (7-14) is simplified further to:

$$E_z = -j\frac{2\eta I_0}{4\pi}\left(\frac{e^{-jkR}}{R}\right) = -j60\frac{e^{-jkR}}{R} \tag{7-38}$$

The far-field approximation solution is given by (7-15), and simplified further to:

$$E_z = -j\frac{\eta I_0 e^{-jkr}}{2\pi r}\cos\left(\frac{\pi z}{2r}\right) = -j60\frac{e^{-jkr}}{r} \tag{7-39}$$

Examining these two similar expressions, it can be seen readily that the far-field approximation solution does not have frequency dependence, while the exact solution does, because R is a function of L, itself a function of frequency. Figure 7.2.7.1-1 below illustrates the comparison.

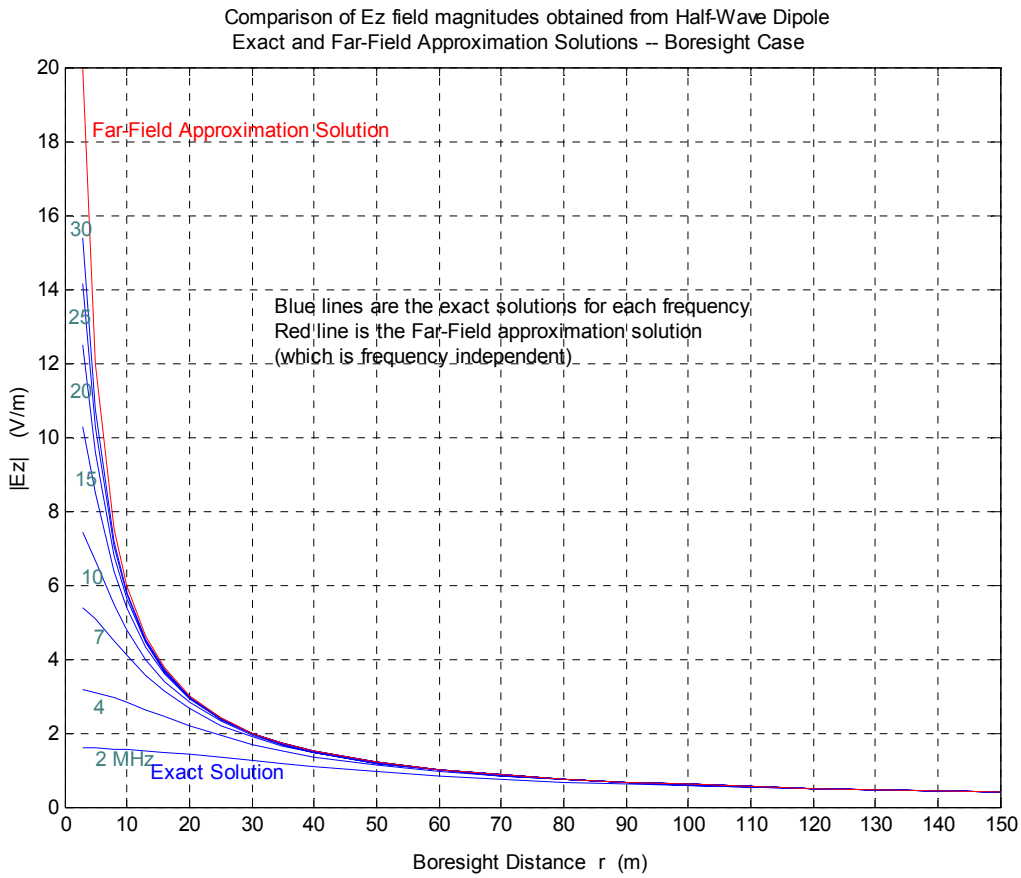

Figure 7.2.7.1-1: Comparison of E_z Magnitudes – Half-Wave Dipole.

7.2.7.2 Full-Wave Dipole Results

For the above set-up, the exact solution given by (7-16) is simplified further to:

$$E_z = -j\frac{2\eta I_0}{4\pi}\left(\frac{e^{-jkR}}{R} + \frac{e^{-jkr}}{r}\right) = -j60\left(\frac{e^{-jkR}}{R} + \frac{e^{-jkr}}{r}\right) \tag{7-40}$$

The far-field approximation solution is given by (7-17), and simplified further to:

$$E_z = -j\frac{2\eta I_0 e^{-jkr}}{2\pi r} = -j120\frac{e^{-jkr}}{r} \tag{7-41}$$

The observation in 7.2.7.1 about the respective frequency dependence of the solutions is equally true similarly, for the observation. Figure 7.2.7.2-1 below illustrates the comparison.

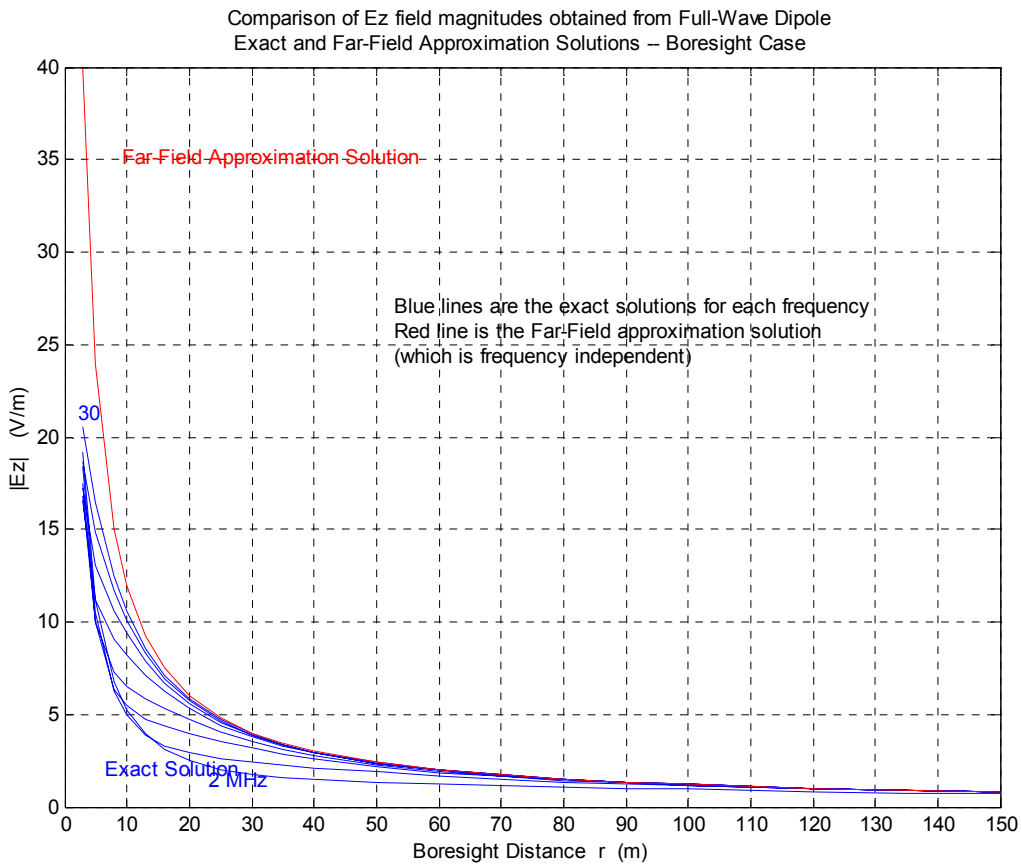

Figure 7.2.7.2-1: Comparison of E_z Magnitudes – Full-Wave Dipole.

7.2.7.3 Comments on Results

Observation: The expressions for E_z are basically Green's Function multiplied by a constant!

It can be seen that near the antenna, the results obtained with the far-field approximation expression will be in error by a considerable margin. Naturally, some distance away from the antenna, the two expressions yield similar results. Also, the frequency dependence disappears because with increasing r, both R and r become comparable in length.

In the HF range, at some distance away from the antenna, the far-field approximation solution is very suitable. On the other hand, near the antenna, the exact expression should always be used for accurate results.

7.3 RECOMMENDED EIRP ESTIMATION METHODS

In the computation of cumulative effects of PLT transmissions, the Task Group recommends that these be computed always using a source defined in terms of EIRP rather than in terms of electric field strength. The cumulative effects assessment described in Chapter 8 use EIRP values.

If the EIRP of the PLT is not known, then the electric field strength could be obtained by means of expressions (7-6) or (7-11) in general, or by means of expressions (7-14) and (7-15) respectively, if a half-wave dipole is selected as a model for the PLT. Then the EIRP could readily be obtained from the following conventional expression:

$$\mathrm{EIRP} = \frac{\left(E(r) * r\right)^2}{30} \tag{7-42}$$

where E(r) is in V/m, r is in metres, 30 is in ohms, and EIRP is in Watts.

If the source is defined in terms of injected PSD, the EIRP per unit bandwidth is the product of the injected PSD and antenna gain. The Task Group recommends using an antenna gain of –30 dBi for In-House systems, –15 dBi for overhead Access systems, and –50 dBi for underground Access systems.

The use of the EIRP determination formula provided in Annex 4 of [3],

$$\mathrm{EIRP} = \frac{r^4}{r^2 + \left(\frac{\lambda}{2\pi}\right)^2} \frac{\left[E(r)\right]^2}{30} = \frac{r^2}{1 + \left(\frac{\left(\frac{\lambda}{2\pi}\right)^2}{r^2}\right)} \frac{\left[E(r)\right]^2}{30} \qquad \left(r \geq \frac{\lambda}{2\pi}\right) \tag{7-43}$$

where E(r) is in V/m, r and λ are in metres, 30 is in ohms, and EIRP is in Watts, is not recommended for Access PLT systems, due to the following reasons:

a) In Annex 4, one critical piece of information is left out. $\frac{\lambda}{2\pi}$ is the far-field boundary (the end of near-field) for electrically-small antennas (i.e., largest dimension < wavelength) such as dipoles. Because (7-43) is a far-field expression, there should have been a qualifier next to it in Annex 4, such as ($r \geq \frac{\lambda}{2\pi}$), as shown above.

b) It can be seen that, when $r \gg \frac{\lambda}{2\pi}$, the results obtained by (7-42) and (7-43) will be very similar. However, when r and $\frac{\lambda}{2\pi}$ are comparable, the results from (7-43) will be in error, from 50% (when $r = \frac{\lambda}{2\pi}$) to some small %. Even when r is at several times the boundary distance, there will be significant error.

7.4 DISTANCE CONVERSION FACTOR NEAR PLT

In this section, measured and modelled distance conversion factors are presented.

The measurement data are from various sources, while the modelling results are obtained from half-wave and full-wave dipole models.

7.4.1 Documented Measurements and Regulatory Conversion Factors

The following conversion factors are from various sources:

a) Ofcom – Ascom PLT Measurements in Winchester [39]:

4.4 MHz:	1 to 3 metres	20 dB/decade
	1 to 10 metres	25 dB/decade
	1 to 30 metres	25 dB/decade
19.8 MHz:	1 to 3/10/30/100 m	20 dB/decade
25.2 MHz:	1 to 3/10/30/100 m	23 dB/decade
Section 6:	< 30 MHz 1 to 100 m	20 dB/decade

b) Ofcom – Amperion PLT Measurements in Crieff [40]:

20 – 23.5 MHz:	Magnetic Field Emission	1 to 30 m	28 dB/decade
		1 to 100 m	28 dB/decade
		1 to 300 m	27 dB/decade
	Electric Field Emission	1 to 30 m	16 dB/decade
		1 to 100 m	21 dB/decade
		1 to 300 m	17 dB/decade
Section 6: < 30 MHz	Magn. Field Em.	1 to 300 m	27 dB/decade
	Electr. Field Em.	1 to 300 m	10 – 21 dB/decade
	Values below 20 dB/decade due to reflections.		

c) VERON EMC Committee [79]:

Outside field strength measurements in the NL at 10 m and 20 m from the house wall were related to averaged In-House measurements at 3 m distance to power lines according to NB 30 rules. The mean variations of field strength with distance for different frequencies were ([79] – Table 8, Figures 7 and 8) between 37.5 dB/decade at 1.84 MHz and 12.0 dB/decade at 28.4 MHz. Further, in General Conclusions, it is stated "These wide spectrum signals have a roll-off of 20 dB/decade…".

d) The University of Karlsruhe made field strength measurements at different distances from 3 m to 110 m to PLT In-House systems [7],[87]. The mean variations of field strength with distance for frequencies below 6 MHz were 25 – 30 dB/decade, and for frequencies higher than 6 MHz 20 dB/decade of distance.

e) The German "Specification for the Measurement of Disturbance Fields…" [12] recommends 3 m as standard distance for NB 30 limits (magnetic field strength measurement). For smaller distances down to 1 m the conversion factor is 20 dB/decade. For greater distances than 3 m the conversion factor should be estimated by measuring at two or more (if necessary) distances, and linear interpolation in a logarithmic plot of field strength over distance.

f) FCC in the United States specifies 40 dB/decade for slant ranges up to 30 metres, below 30 MHz [31],[90]. It should be noted that this conversion factor has been questioned by several authors, e.g., [98],[99].

7.4.2 Results from Modelling Calculations

To determine the distance conversion factor theoretically, the exact solution expression for E_z is used, as the far-field approximation expression will not be suitable in the vicinity of the PLT line. The PLT line is

horizontal. The two-ray technique described in Section 7.2.6 is utilized. The boresight case is applied (z = 0) which yields the maximum E_z values. The line current I_0 is 1 ampere. Both half-wavelength (half-wave or $\lambda/2$) and one-wavelength (full-wave or λ) dipoles are modelled.

When z = 0, R1 = R2 = R and is given by (7-24), and r is the radial distance from the centre of the dipole, in the boresight direction, and is given by (7-23). L is the dipole length.

PLT line was placed at two heights, H1 at 10 and 15 metres above ground. These heights represent the typical PLT line height range above ground. The observation point H2 was placed at 1 metre above ground. The horizontal distance from PLT line, D, varied from 1 to 300 metres, in 1 metre increments. The direct and reflected path expressions for r, R1 and R2 are given by (7-29) through (7-31). **Note**: r_dir, (7-29), is the so-called slant range in the FCC documents. The horizontal reflection coefficient Γ_H is given by (7-35). Six frequencies were used: 2, 3, 5, 10, 20, 30 MHz, with $\varepsilon_r = 15$, and $\sigma = 0.005$. The total E_z field magnitude was obtained by using (7-36) and (7-37). Finally, both half-wave and full-wave dipole models were utilized.

All of the results are plotted against r_dir, the slant range between the PLT line and observation point. Furthermore, for comparison purposes, the single-ray case is also shown, which is actually the magnitude of E_z obtained by the direct path.

7.4.2.1 Horizontal Reflection Coefficient Profile

The horizontal reflection coefficient Γ_H behaviour is independent of the dipole model used. Therefore, the following profiles apply equally to both half-wave and full-wave dipole models. Figures 7.4.2.1-1 and 7.4.2.1-2 show the horizontal reflection coefficient real and imaginary parts, for PLT line heights of 10 and 15 metres, respectively. As mentioned before in Section 7.2.6, the air/ground medium is the case here, and the results are obtained from Equation (7-35).

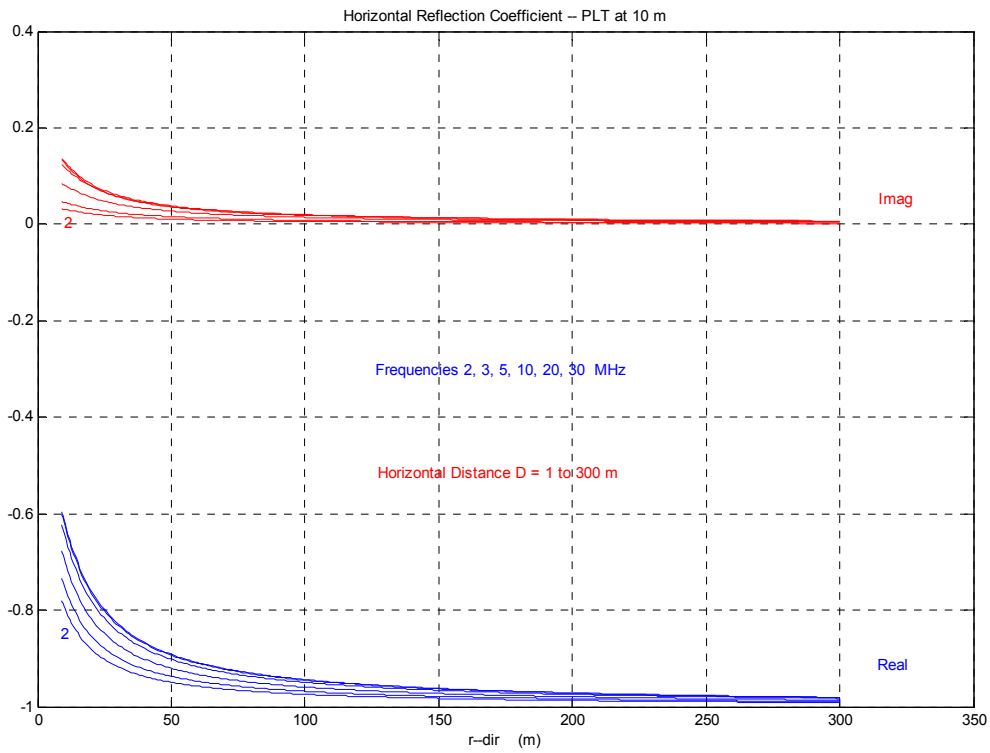

Figure 7.4.2.1-1: Horizontal Reflection Coefficient Profile – PLT Line Height at 10 Metres.

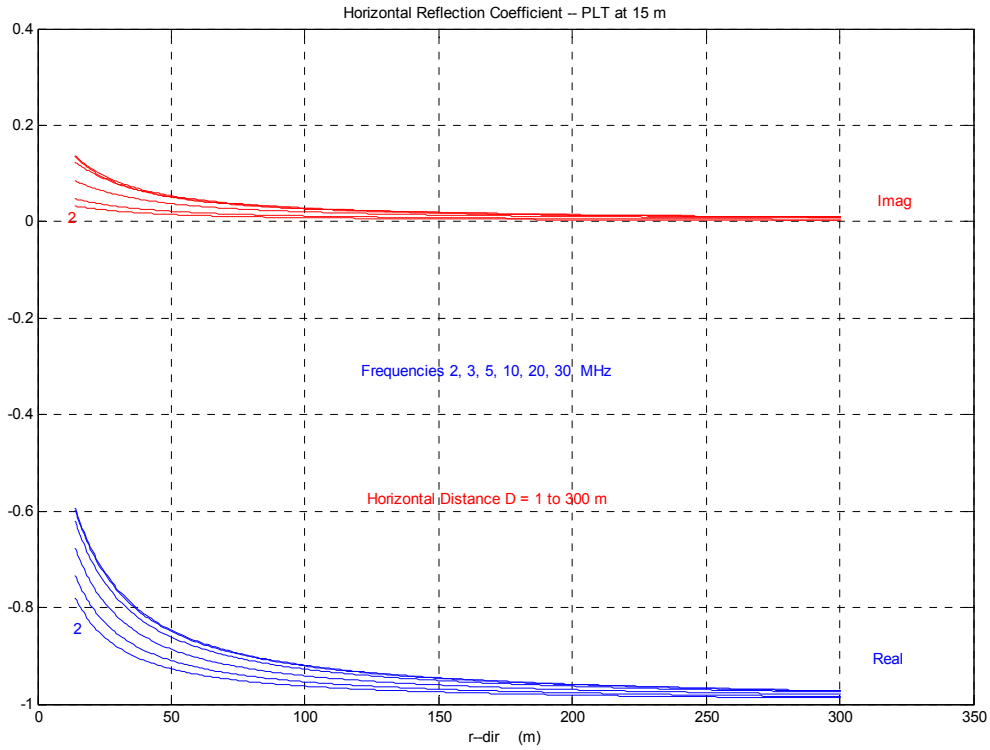

Figure 7.4.2.1-2: Horizontal Reflection Coefficient Profile – PLT Line Height at 15 Metres.

7.4.2.2 Half-Wave Dipole Results

The general exact expression used for E_z is given by (7-38). The results obtained are plotted in the following Figures. Figures 7.4.2.2-1 to 7.4.2.2-3 show the two-ray, single-ray and combined plots, respectively, when PLT line is at 10 metres above ground. Figures 7.4.2.2-4 to 7.4.2.2-6 show the two-ray, single-ray and combined plots, respectively, when PLT line is at 15 metres above ground.

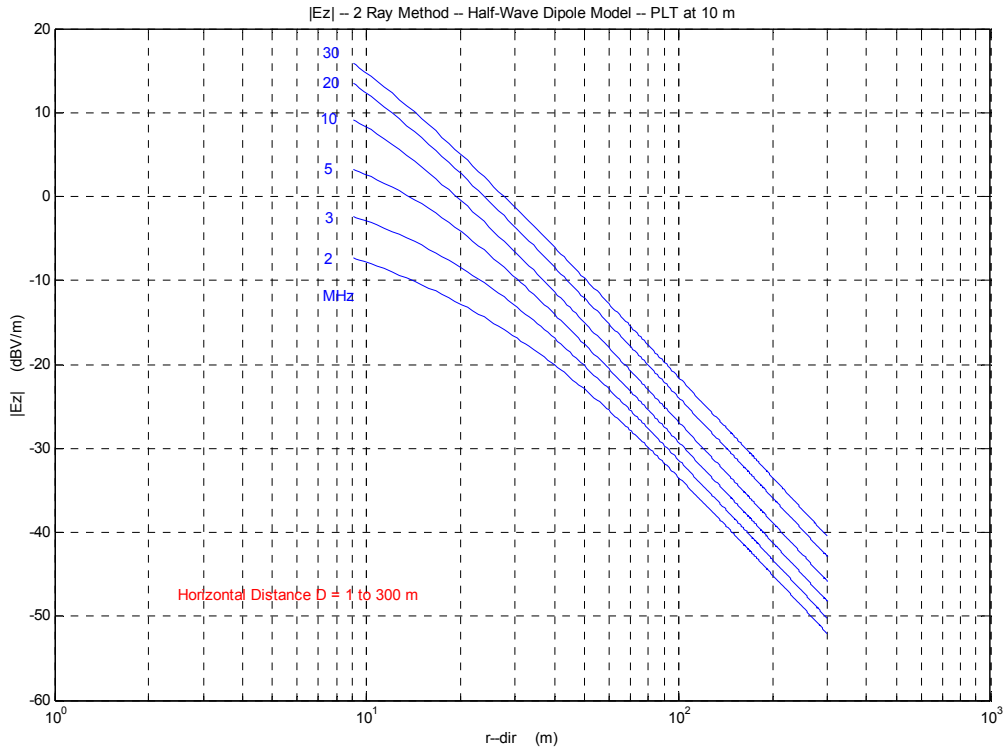

Figure 7.4.2.2-1: Two-Ray Results – PLT Line Height at 10 Metres – L = λ/2.

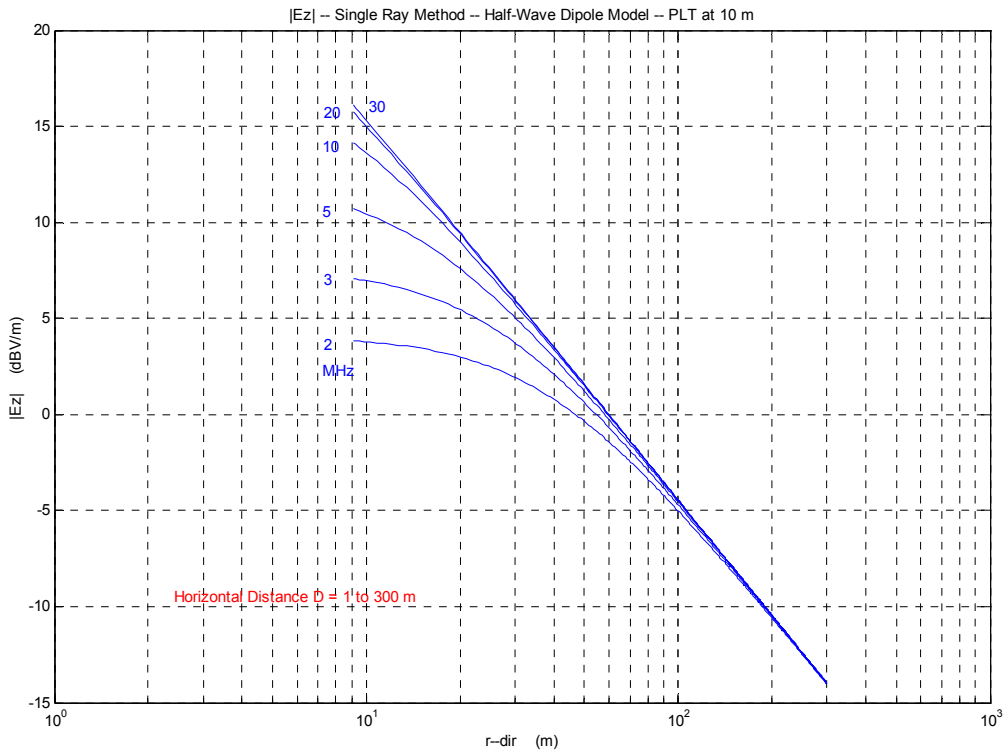

Figure 7.4.2.2-2: Single-Ray Results – PLT Line Height at 10 Metres – L = λ/2.

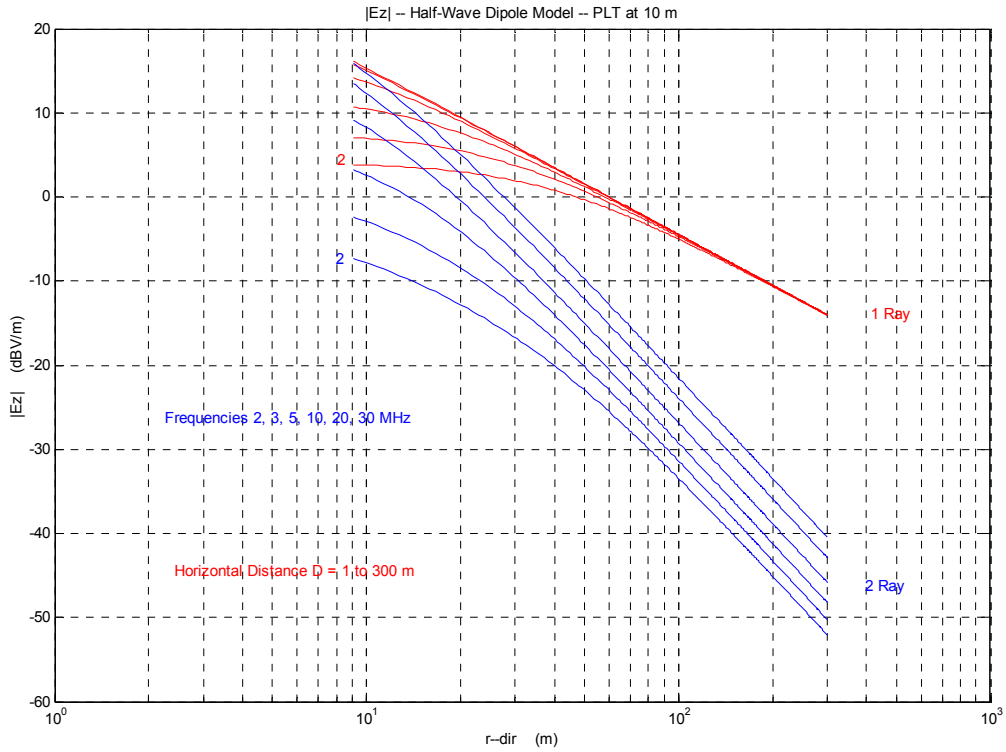

Figure 7.4.2.2-3: Combined Results – PLT Line Height at 10 Metres – L = λ/2.

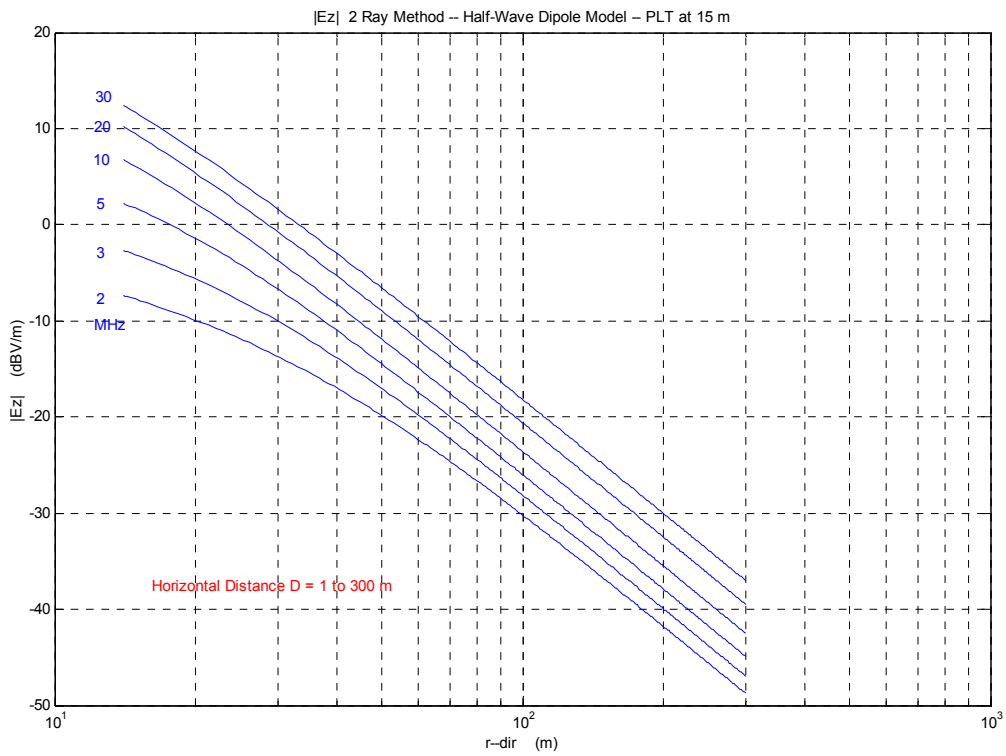

Figure 7.4.2.2-4: Two-Ray Results – PLT Line Height at 15 Metres – L = λ/2.

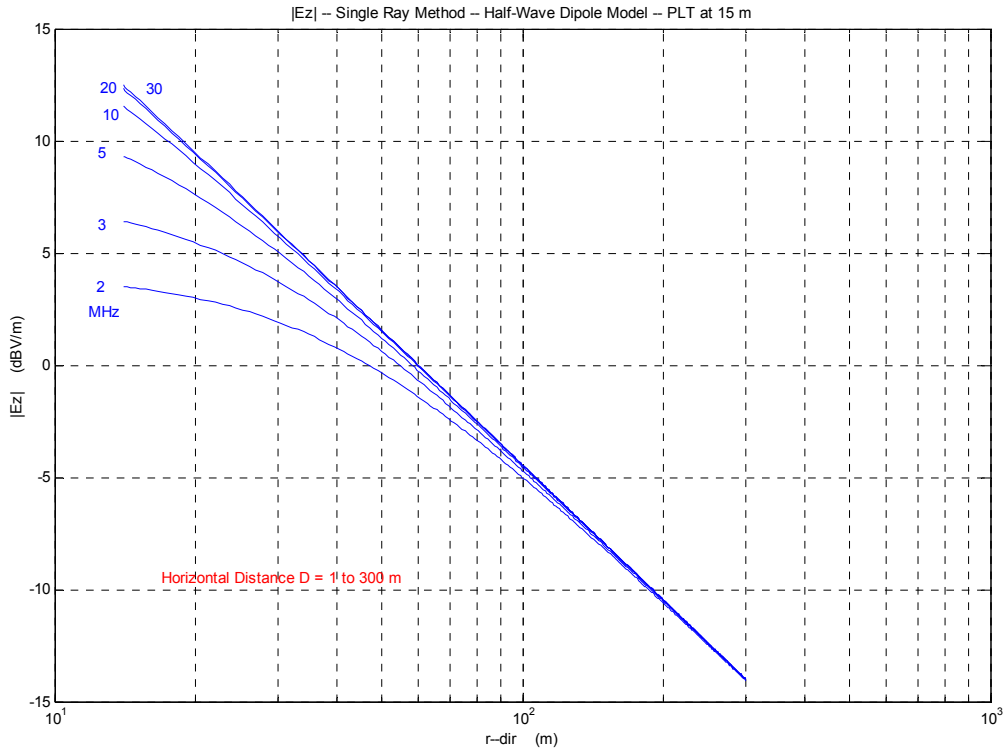

Figure 7.4.2.2-5: Single-Ray Results – PLT Line Height at 15 Metres – L = λ/2.

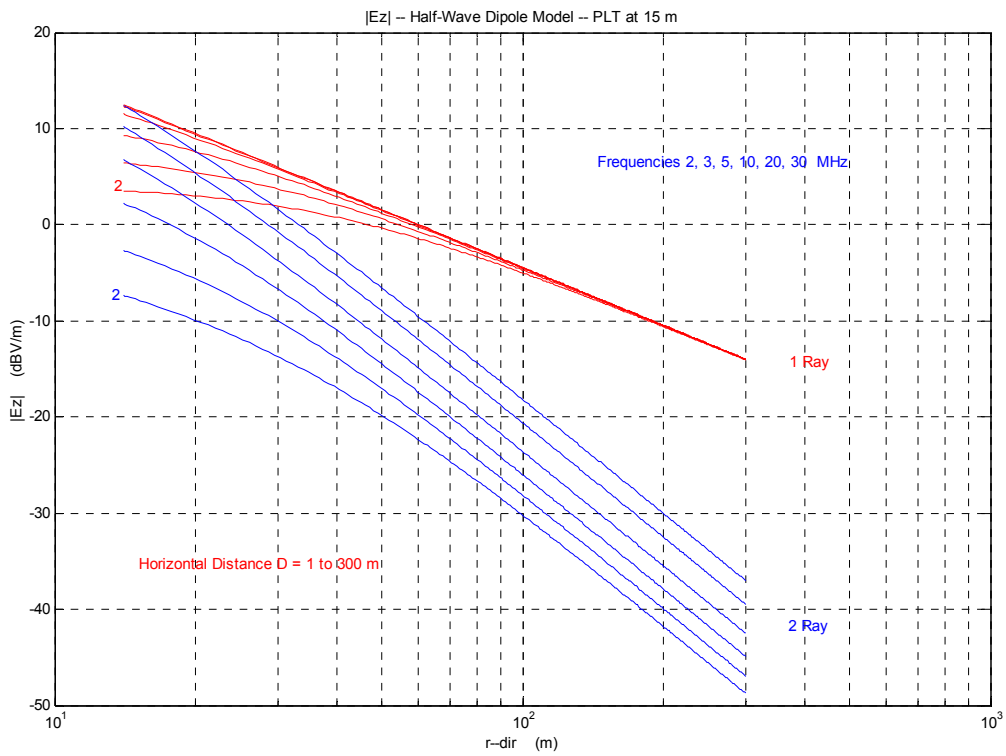

Figure 7.4.2.2-6: Combined Results – PLT Line Height at 15 Metres – L = λ/2.

7.4.2.3 Full-Wave Dipole Results

The general exact expression used for E_z is given by (7-40). The results obtained are plotted in the following Figures. Figures 7.4.2.3-1 to 7.4.2.3-3 show the two-ray, single-ray and combined plots, respectively, when PLT line is at 10 metres above ground. Figures 7.4.2.3-4 to 7.4.2.3-6 show the two-ray, single-ray and combined plots, respectively, when PLT line is at 15 metres above ground.

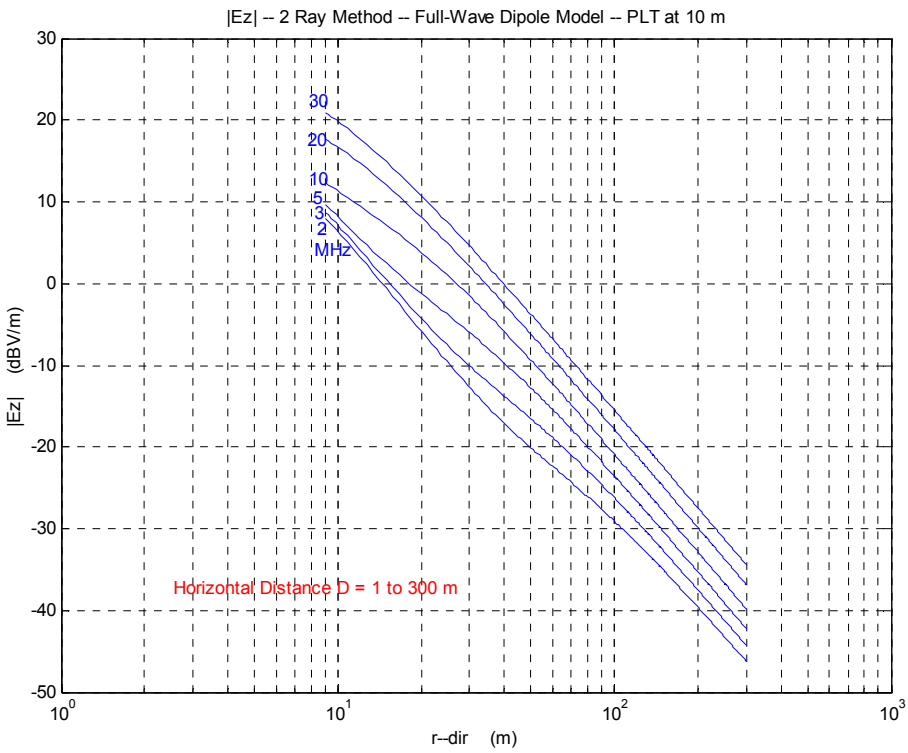

Figure 7.4.2.3-1: Two-Ray Results – PLT Line Height at 10 Metres – L = λ.

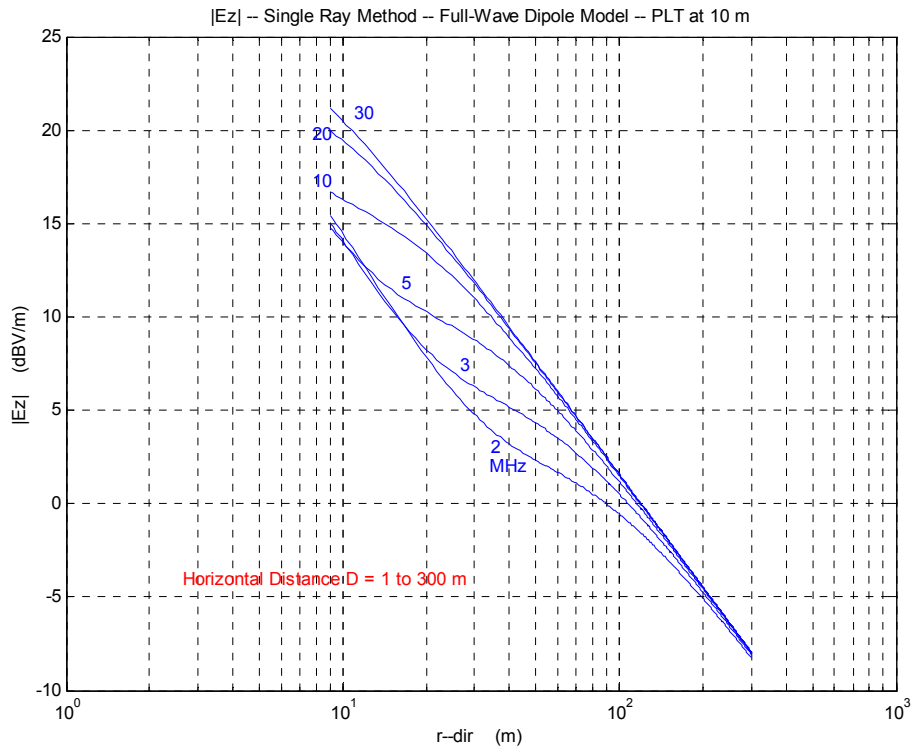

Figure 7.4.2.3-2: Single-Ray Results – PLT Line Height at 10 Metres – L = λ.

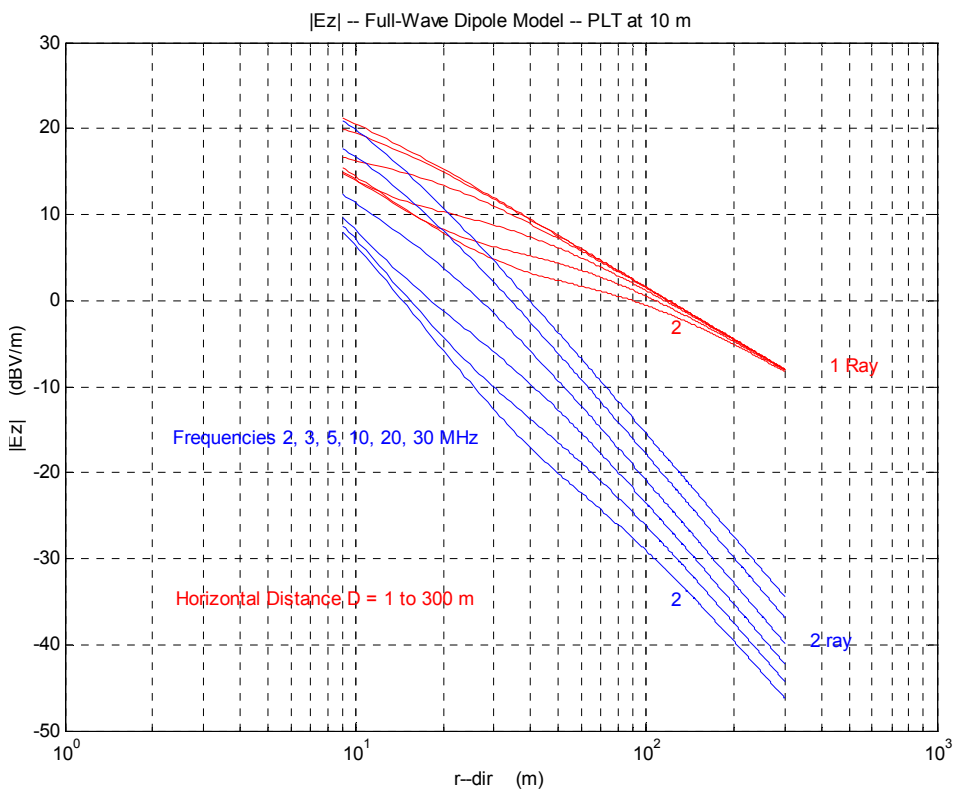

Figure 7.4.2.3-3: Combined Results – PLT Line Height at 10 Metres – L = λ.

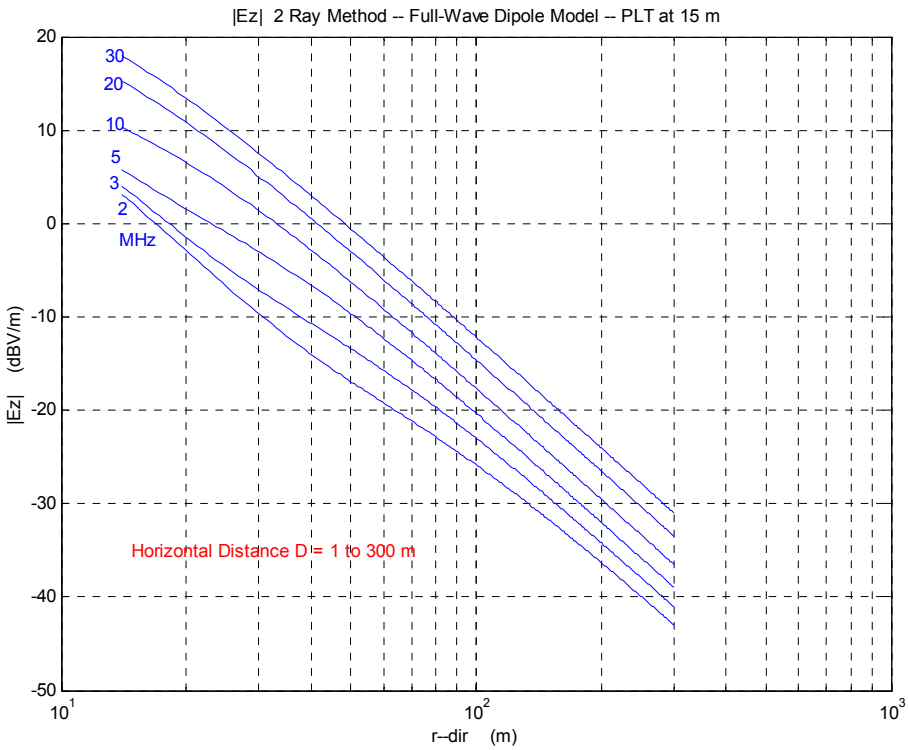

Figure 7.4.2.3-4: Two-Ray Results – PLT Line Height at 15 Metres – L = λ.

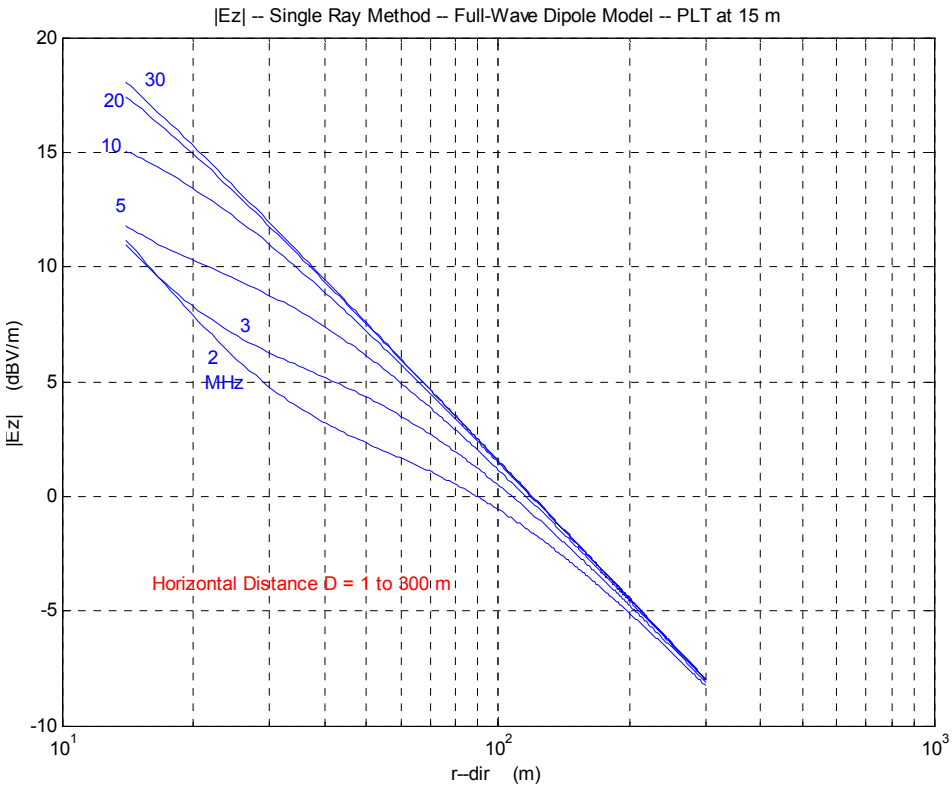

Figure 7.4.2.3-5: Single-Ray Results – PLT Line Height at 15 Metres – L = λ.

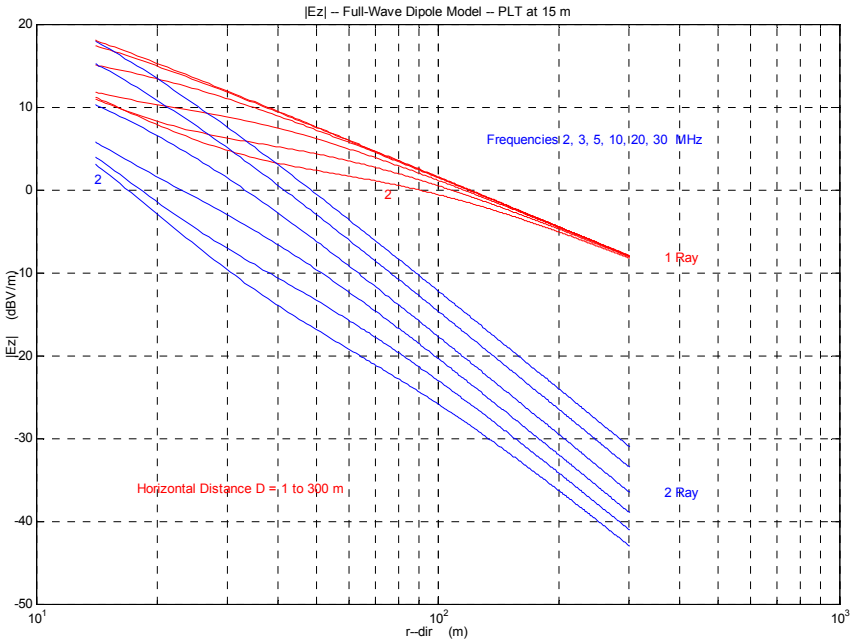

Figure 7.4.2.3-6: Combined Results – PLT Line Height at 15 Metres – L = λ.

7.4.2.4 Comments on Results

The following comments can be made about the above results:

a) For the horizontal polarization case as we have with the PLT line, the total E_z field magnitude obtained with the two-ray method will always be smaller than for the single-ray approach, because of the effect of the reflection coefficient (negative real part predominates).

b) The effects of geometry (D, H1, H2) and frequency on the reflection coefficient is the reason why there is a family of curves with the two-ray method, and, unlike the case for the single-ray, they do not converge within the calculation range utilized here.

c) In the single-ray case, the results are practically indistinguishable, with the minor differences due to PLT line heights of 10 and 15 metres. At some distance away from the antenna, E_z varies inversely with r_dir (20 dB/decade), and as expected, the frequency dependence disappears. It is logical to take 200 metres as this limit, as indicated in Section 7.2.6, last paragraph.

d) Obviously, near the antenna, the two-ray case will be in force. At some distance away, the single-ray case will be applicable. Therefore, the distance conversion factor will have to be a composite of the two cases.

7.4.3 Determination of Distance Conversion Factor

To obtain the distance conversion factor, we can use the following expression:

$$|E_z|(1) + X*\log_{10}[r_dir(1)/r_dir(2)] = |E_z|(2) \text{ or}$$

$$X = \{|E_z|(2) - |E_z|(1)\}/ \log_{10}[r_dir(1)/r_dir(2)] \qquad (7\text{-}45)$$

where X is the distance conversion factor in dB/decade.

7.4.3.1 Half-Wave Model

From the MATLAB results for Figures 7.4.2.2-1 and 7.4.2.2-4, the following information is excised to help identify the distance conversion factor figures. The numbers under the frequencies are the values of $|E_z|$ in dBV/m. The * in the Tables indicates extrapolated numbers read off the Figures 7.4.2.2-1 and 7.4.2.2-4 (from the original MATLAB large-size graphs).

Table 7.4.3.1-1: $|E_z|$ Values (dBV/m) – PLT Line at 10 Metres – L = λ/2

r_dir (m)	2 MHz	3 MHz	5 MHz	10 MHz	20 MHz	30 MHz
9.05	-7.31	-2.38	3.27	9.19	13.48	15.88
20.13	-12.86	-8.49	-4.22	-0.53	2.62	4.95
30.37	-16.87	-13.18	-9.81	-6.84	-3.88	-1.52
49.82	-22.93	-20.12	-17.53	-14.97	-12.07	-9.69
100.40	-33.51	-31.44	-29.30	-26.90	-23.98	-21.58
200.20	-45.07	-43.23	-41.19	-38.81	-35.87	-33.44
300.14	-52.04	-50.23	-48.21	-45.83	-42.87	-40.44
500.00*	-60.9	-59.0	-57.1	-54.8	-51.4	-49.0

Table 7.4.3.1-2: $|E_z|$ Values (dBV/m) – PLT Line at 15 Metres – L = λ/2

r_dir (m)	2 MHz	3 MHz	5 MHz	10 MHz	20 MHz	30 MHz
14.04	-7.37	-2.70	2.24	6.75	10.19	12.41
19.80	-9.86	-5.52	-1.29	2.37	5.51	7.80
30.41	-13.85	-10.20	-6.88	-3.94	-0.95	1.40
50.00	-19.82	-17.04	-14.47	-11.92	-8.97	-6.57
99.99	-30.20	-28.13	-25.99	-23.58	-20.60	-18.16
200.49	-41.82	-39.98	-37.94	-35.53	-32.52	-30.06
300.33	-48.76	-46.96	-44.93	-42.51	-39.49	-37.02
500.00*	-57.2	-55.8	-53.8	-51.5	-48.5	-46.0

Table 7.4.3.1-3: Distance Conversion Factors – PLT Line at 10 Metres – L = λ/2

r_dir (1)	r_dir (2)	2 MHz	3 MHz	5 MHz	10 MHz	20 MHz	30 MHz
9.05	20.13	16.0	17.6	21.6	28.0	31.3	31.5
20.13	30.37	22.5	26.3	31.3	35.3	36.4	36.2
20.13	100.40	29.6	32.9	35.9	37.8	38.1	38.0
20.13	200.20	32.3	34.8	37.1	38.4	38.6	38.5
30.37	100.40	32.0	35.2	37.5	38.6	38.7	38.6
30.37	300.14	35.4	37.2	38.6	39.2	39.2	39.1
49.82	500.00*	37.9	38.8	39.5	39.8	39.3	39.3

Table 7.4.3.1-4: Distance Conversion Factors – PLT Line at 15 Metres – L = λ/2

r_dir (1)	r_dir (2)	2 MHz	3 MHz	5 MHz	10 MHz	20 MHz	30 MHz
14.04	19.80	16.7	18.9	23.6	29.3	31.4	30.9
19.80	30.41	21.4	25.1	30.0	33.9	34.7	34.3
19.80	99.99	28.9	32.2	35.1	36.9	37.1	36.9
19.80	200.49	31.8	34.3	36.5	37.7	37.8	37.7
30.41	99.99	31.6	34.7	37.0	38.0	38.0	37.8
30.41	300.33	35.1	37.0	38.3	38.8	38.8	38.6
50.00	500.00*	37.4	38.8	39.3	39.6	39.5	39.4

It can readily be seen that the PLT line height does not affect the distance conversion factor results appreciably. Therefore, the values in Tables 7.4.3.1-3 and 7.4.3.1-4 can be averaged to obtain typical values, as shown in Table 7.4.3.1-5.

Table 7.4.3.1-5: Averaged Distance Conversion Factors – L = λ/2

r_dir (m)	2 MHz	3 MHz	5 MHz	10 MHz	20 MHz	30 MHz
Up to 20	16.4	18.3	22.6	28.7	31.4	31.2
20 – 30	22.0	25.7	30.7	34.6	35.6	35.3
20 – 100	29.3	32.6	35.5	37.4	37.6	37.5
20 – 200	32.1	34.6	36.8	38.1	38.2	38.1
30 – 100	31.8	35.0	37.3	38.3	38.4	38.2
30 – 300	35.3	37.1	38.5	39.0	39.0	38.9
50 – 500	37.7	38.8	39.4	39.7	39.4	39.4

A careful review indicates that these averaged results can be further refined into four zones in terms of slant range and frequency, as shown in Table 7.4.3.1-6 (values are in dB/decade):

Table 7.4.3.1-6: Distance Conversion Factors (dB/decade) – L = λ/2

Zone (m)	2 MHz	3 MHz	5 MHz	10 – 30 MHz
r_dir ≤ 20	16	18	23	29 - 31
20 < r_dir ≤ 30	22	26	31	35
30 < r_dir ≤ 200	32	35	37	38
r_dir > 200	20	20	20	20

Beyond 200 metres, the single-ray method and its factor (20 dB/decade) is applicable, as mentioned in Section 7.4.2.4, paragraph c).

7.4.3.2 Full-Wave Model

From the MATLAB results for Figures 7.4.2.3-1 and 7.4.2.3-4, the following information is excised to help identify the distance conversion factor figures. The numbers under the frequencies are the values of $|E_z|$ in dBV/m. The * in the Tables indicates extrapolated numbers read off the Figures 7.4.2.3-1 and 7.4.2.3-4 (from the original MATLAB large-size graphs).

Table 7.4.3.2-1: $|E_z|$ Values (dBV/m) – PLT Line at 10 Metres – L = λ

r_dir (m)	2 MHz	3 MHz	5 MHz	10 MHz	20 MHz	30 MHz
9.05	7.99	8.72	9.61	12.30	17.65	20.88
20.13	-5.87	-4.36	-1.26	3.78	8.07	10.71
30.37	-12.93	-10.28	-6.18	-1.73	1.88	4.37
49.82	-20.06	-16.51	-12.74	-9.33	-6.15	-3.72
100.40	-29.13	-26.29	-23.63	-20.98	-17.99	-15.57
200.20	-39.57	-37.45	-35.26	-32.82	-29.85	-27.42
300.14	-46.26	-44.32	-42.23	-39.82	-36.85	-34.42
500.00*	-54.5	-53.1	-51.0	-48.8	-45.7	-43.1

Table 7.4.3.2-2: $|E_z|$ Values (dBV/m) – PLT Line at 15 Metres – L = λ

r_dir (m)	2 MHz	3 MHz	5 MHz	10 MHz	20 MHz	30 MHz
14.04	3.10	4.02	5.77	10.26	15.22	17.95
19.80	-2.75	-1.32	1.67	6.66	10.96	13.55
30.41	-9.91	-7.29	-3.23	1.18	4.81	7.30
50.00	-16.94	-13.41	-9.67	-6.27	-3.05	-0.59
99.99	-25.84	-22.99	-20.33	-17.65	-14.61	-12.16
200.49	-36.32	-34.20	-32.01	-29.53	-26.51	-24.04
300.33	-42.98	-41.05	-38.95	-36.50	-33.47	-31.00
500.00*	-51.3	-49.2	-47.5	-44.7	-41.9	-39.4

Table 7.4.3.2-3: Distance Conversion Factors – PLT Line at 10 Metres – L = λ

r_dir (1)	r_dir (2)	2 MHz	3 MHz	5 MHz	10 MHz	20 MHz	30 MHz
9.05	20.13	39.9	37.7	31.3	24.5	27.6	29.3
20.13	30.37	39.5	33.2	27.6	30.9	34.7	35.5
20.13	100.40	33.3	31.4	32.1	35.5	37.3	37.7
20.13	200.20	33.8	33.2	34.1	36.7	38.0	38.2
30.37	100.40	31.2	30.8	33.6	37.1	38.3	38.4
30.37	300.14	33.5	34.2	36.2	38.3	38.9	39.0
49.82	500.00*	34.4	36.5	38.2	39.4	39.5	39.3

Table 7.4.3.2-4: Distance Conversion Factors – PLT Line at 15 Metres – L = λ

r_dir (1)	r_dir (2)	2 MHz	3 MHz	5 MHz	10 MHz	20 MHz	30 MHz
14.04	19.80	39.2	35.8	27.5	24.1	28.5	29.5
19.80	30.41	38.4	32.0	26.3	29.4	33.0	33.5
19.80	99.99	32.8	30.8	31.3	34.6	36.4	36.6
19.80	200.49	33.4	32.7	33.5	36.0	37.3	37.4
30.41	99.99	30.8	30.4	33.1	36.4	37.6	37.6
30.41	300.33	33.3	33.9	35.9	37.9	38.5	38.5
50.00	500.00*	34.4	35.8	37.8	38.4	38.9	38.8

Again, it can readily be seen that the PLT line height does not affect the distance conversion factor results appreciably. Therefore, the values in Tables 7.4.3.2-3 and 7.4.3.2-4 can be averaged to obtain typical values, as shown in Table 7.4.3.2-5.

Table 7.4.3.2-5: Averaged Distance Conversion Factors – L = λ

r_dir (m)	2 MHz	3 MHz	5 MHz	10 MHz	20 MHz	30 MHz
Up to 20	39.6	36.8	29.4	24.3	28.1	29.4
20 – 30	39.0	32.6	27.0	30.2	33.9	34.5
20 – 100	33.1	31.1	31.7	35.1	36.9	37.2
20 – 200	33.6	33.0	33.8	36.4	37.7	37.8
30 – 100	31.0	30.6	33.4	36.8	38.0	38.0
30 – 300	33.4	34.1	36.1	38.1	38.7	38.8
50 – 500	34.4	36.2	38.0	38.9	39.2	39.1

The contents of Table 7.4.3.2-5 can be further refined into four zones in terms of slant range and frequency, as shown in Table 7.4.3.2-6 (values are in dB/decade). However, the full-wave model exhibits more complicated results, as seen in the figures of Section 7.4.2.3.

Table 7.4.3.2-6: Distance Conversion Factors (dB/decade) – L = λ

Zone (m)	2 MHz	3 MHz	5 MHz	10 MHz	20 – 30 MHz
r_dir ≤ 20	40	37	29	24	28 – 29
20 < r_dir ≤ 30	39	33	27	30	34
30 < r_dir ≤ 200	31 – 33	31 – 33	33	36	38
r_dir > 200	20	20	20	20	20

Beyond 200 metres, the single-ray method and its factor (20 dB/decade) is applicable, as mentioned in Section 7.4.2.4, paragraph c).

One important observation is that the E_z field magnitudes obtained with full-wave dipole model are several dB higher than those obtained with the half-wave dipole model. The reason for this is the higher directivity of the full-wave dipole due to its narrower beamwidth.

7.4.4 Remarks

As indicated in Section 7.2, the half-wave dipole is preferable to the full-wave dipole as a modelling tool. Accordingly, the distance conversion factors listed in Table 7.4.3.1-6 are selected for the theoretical results.

A direct comparison of measured and theoretical results is not practical due to the many uncertainties involved in the various measurement techniques, instruments, positional (locational) variables, and so on.

It should also be noted that some of the measurement results shown in Section 7.4.1 are for In-House systems and are not comparable. Nevertheless, both sets of results show a commonality of values and similar variation with frequency and distance.

7.5 REPRESENTATIVE PLT SOURCES

In order to be able to predict cumulative effects of PLT in Chapter 8, the EIRP of PLT systems must be estimated. Below, different values are proposed for use in this regard.

Based on injected PSD:

- HomePlug systems (1.0 or AV): Injected PSD –50 dBm/Hz, antenna gain –30 dBi, average duty cycle 30% (considering the multitude of usages for an In-House network; media distribution, computer networking, etc.).
- Amperion Access system: Injected PSD –50 dBm/Hz, antenna gain –15 dBi, average duty cycle 15%.

Based on limits (see Chapter 4 for numerical values, and then use conversion methods recommended in Section 7.3 to obtain EIRP):

- NB30.
- FCC Part 15.
- Proposed European common mode current limits are not applicable, as no method to estimate EIRP from common mode current has been properly established.